

Emission of SN 1006 produced by accelerated cosmic rays

E.G.Berezhko¹, L.T.Ksenofontov¹, and H.J.Völk²

¹ Institute of Cosmophysical Research and Aeronomy, 31 Lenin Ave., 677891 Yakutsk, Russia
e-mail: berezhko@ikfia.ysn.ru e-mail: ksenofon@ikfia.ysn.ru

² Max Planck Institut für Kernphysik, Postfach 103980, D-69029 Heidelberg, Germany
e-mail: Heinrich.Voelk@mpi-hd.mpg.de

Received month day, year; accepted month day, year

Abstract. The nonlinear kinetic model of cosmic ray (CR) acceleration in supernova remnants (SNRs) is used to describe the properties of the remnant of SN 1006. It is shown, that the theory fits the existing data in a satisfactory way within a set of parameters which is consistent with the idea that SN 1006 is a typical Galactic CR source. The adjusted parameters are those that are not very well determined by present theory or not directly amenable to astronomical observations. The calculated expansion law and the radio-, X-ray and γ -ray emissions produced by the accelerated CRs in SN 1006 agree quite well with the observations. A quite large interior magnetic field $B_d \approx 100 \mu\text{G}$ is required to give a good fit for the radio and X-ray synchrotron emission. In the observed TeV γ -ray flux from SN 1006, the π^0 -decay γ -rays, generated by the nuclear CR component, dominate over the inverse Compton (IC) γ -rays, generated by the CR electrons in the cosmic microwave background. The predicted integral γ -ray flux $F_\gamma \propto \epsilon_\gamma^{-1}$ extends up to energies $\sim 100 \text{ TeV}$ if CR diffusion is as strong as the Bohm limit. Only if the interior magnetic field is much lower, $B_d \approx 10 \mu\text{G}$, then the observed γ -ray emission is due to the accelerated electron component alone. In this case, less plausible physically in our view, the upper limit of the proton to electron ratio is so low (less than 5), and their maximum individual energy and total energy content so small, that SN 1006 can not be considered as a typical source of the Galactic CRs.

Key words. theory – cosmic rays – shock acceleration – supernova remnants (SN 1006) – radiation: radioemission – X-rays – gamma-rays

1. Introduction

In the last years significant efforts have been made to obtain direct observational evidence whether the Galactic cosmic rays (CRs) are indeed generated in supernova remnants (SNRs). The expected π^0 -decay γ -ray emission, produced in nearby SNRs by the accelerated protons in their collisions with thermal gas nuclei, is marginally high enough to be detectable by the present generation of imaging atmospheric Cherenkov telescopes (e.g. Drury et al. 1994; Berezhko & Völk 1997). Positive results of such observations would constitute a necessary condition for a dominant role of SNRs in the production of the Galactic CRs and of their energy spectrum.

The results of recent nonthermal X-ray and γ -ray observations indicate that at least CR electrons are accelerated in SNRs. SN 1006 is one of the SNRs for which there is evidence that electrons reach energies of about 100 TeV (Koyama et al. 1995; Tanimori et al. 1998, 2001). It is also one of the three shell type SNRs in which TeV γ -ray emission has been detected up to now. However, the

interpretation of these data is not unique. Depending on the assumed values for the unknown physical parameters of SN 1006 (mainly the value of the magnetic field, the electron to proton ratio, and the nucleon injection rate), the observed high-energy γ -ray emission can be predominantly either inverse Compton (IC) radiation due to CR electrons scattering on the microwave background radiation (as predicted from the X-ray synchrotron emission by Pohl 1996, Mastichiadis & de Jager 1996, and Yoshida & Yanagita 1997), or π^0 -decay emission due to hadronic collisions of CRs with gas nuclei (Aharonian & Atoyan 1999; Berezhko et al. 1999, 2001).

The thermal and nonthermal X-ray emission has recently been rediscussed by Allen et al. (2001) who draw phenomenological conclusions on the γ -ray emission to be dominated by IC radiation as well as on the production and the characteristics of the nonthermal nucleonic particle component which they estimate to have a total energy of 10^{50} ergs.

In contrast, our starting point is the overall SNR dynamics and the acceleration theory of the nonthermal component. Thus we accept the X-ray results and the

quantitative distinction between thermal X-ray emission and the nonthermal synchrotron components, including the constraints on the external density derived from them. We rather calculate the outer shock size, speed and compression ratio as well as the nonthermal quantities as solutions of the nonlinear, time-dependent kinetic equations for electrons and protons as functions of space, time and particle momentum, rather than phenomenologically assuming forms of the electron and proton momentum distribution functions. In this way we also obtain morphological information. We determine the unknown parameters like the upstream magnetic field strength and the electron to proton ratio, and constrain the nucleon injection rate which is incompletely known from theory, by comparing with the observations. For this purpose we use the self-consistent kinetic model of diffusive acceleration of CRs in SNRs (Berezhko et al. 1996; Berezhko & Völk 1997) and investigate the γ -ray emission from SN 1006.

In contrast to a previous study (Berezhko et al. 1999) we restrict ourselves to the so-called Bohm limit for CR diffusion near the shock, assuming efficient and strong Alfvén wave excitation by the accelerating particles themselves. Our considerations show that, together with a renormalization due to the lack of spherical symmetry of the nucleon injection, the existing data are consistent with very efficient acceleration of CR nuclei at the SN shock wave which converts a significant fraction of the initial SNR energy content into CR energy. This energy is distributed between energetic protons and electrons in a proportion similar to that of the Galactic CRs. Therefore the observed γ -ray emission of SN 1006 can indeed be of hadronic origin, and we consider this as the physically most plausible solution from the point of view of acceleration theory.

Nevertheless, the existing observations do not strongly exclude a solution in which nuclear CRs play no important role and all nonthermal emissions are of leptonic origin. Therefore we analyze whether the existing data can also be fitted by an essentially different set of parameters. We demonstrate that there is an alternative possibility to fit the overall data albeit with somewhat lower quality. It implies a (physically not very plausible) much lower injection rate and acceleration efficiency of protons, a much larger electron to proton ratio, and a lower magnetic field value compared with the case of efficient CR nucleon acceleration. Assuming SN 1006 to be a typical representative, in this second case one can not consider the SNRs as the source population of the Galactic CRs due to the low proton acceleration efficiency. To discriminate empirically between these rather different scenarios γ -ray measurements above 10 TeV are required: in this very high energy range a measurable γ -ray flux is expected only in the case of efficient nucleonic CR production.

2. Model

Since SN 1006 is a type Ia supernova (SN) we suggest that its evolution takes place in a uniform interstellar medium (ISM). The general picture is then well-known.

A SN explosion ultimately ejects a shell of matter with total energy E_{sn} and mass M_{ej} . During an initial period the shell material has a broad distribution in velocity v . The fastest part of these ejecta is described by a power law $dM_{\text{ej}}/dv \propto v^{2-k}$ (e.g. Jones et al. 1981; Chevalier 1982). The interaction of the ejecta with the ISM creates a strong shock there which accelerates particles.

Our nonlinear model (Berezhko et al. 1996; Berezhko & Völk 1997) is based on a fully time-dependent solution of the CR transport equation together with the gas dynamic equations in spherical symmetry.

The CR diffusion coefficient is taken as the Bohm limit

$$\kappa(p) = \kappa(mc)(p/mc), \quad (1)$$

where approximately $\kappa(mc) = mc^2/(3eB)$, e and m are the particle charge and mass, p denotes the particle momentum, B is the magnetic field strength, and c is the speed of light. With this diffusion coefficient we assume that the production of scattering waves is so strong that limitations due to wave refraction (Malkov et al. 2001) do not come in to influence the solution.

The number of suprathermal protons injected into the acceleration process is described by a dimensionless injection parameter η which is a fixed fraction of the ISM particles entering the shock front. For simplicity it is assumed that the injected particles have a velocity four times higher than the postshock sound speed. Unfortunately there is no complete selfconsistent theory of a collisionless shock transition, which can predict the value of the injection rate and its dependence on the shock parameters. For the case of a purely parallel shock hybrid simulation predict a quite high ion injection (e.g. Scholer et al. 1992; Bennet & Ellison 1995) which corresponds to the value $\eta \sim 10^{-2}$ of our injection parameter. Such a high injection is consistent with analytical models (Malkov & Völk 1995, 1996; Malkov 1998) and confirmed by measurements near the Earth's bow shock (Trattner & Scholer 1994). We note however that in our spherically symmetric model these results can only be used with some important modification. In reality we consider the evolution of the large scale SN shock which expands into the ISM with its magnetic field. In the case of SN 1006, at the current evolutionary phase, the shock has a size of several parsecs. On such a scale the unshocked interstellar magnetic field can be considered as uniform since its random component is characterized by a much larger main scale of about 100 pc. Then our spherical shock is quasi-parallel in the polar regions and quasi-perpendicular in the equatorial region. This magnetic field essentially suppresses the leakage of suprathermal particles from the downstream region back upstream when the shock is more and more oblique (Ellison et al. 1995; Malkov & Völk 1995). Applied to the spherical shock in the uniform external magnetic field it would mean that

only small regions near the poles covering less than 10% of the shock surface allow a sufficiently high injection ultimately leading to the transformation of an essential part (more than a few percent) of the shock energy into CR energy, whereas the main part of the shock is an inefficient CR accelerator. If one takes into account the Alfvén wave excitation due to CR streaming (which becomes efficient already at a very low injection rate $\eta \sim 10^{-7}$) the local injection rate has to be averaged over the fluctuating magnetic field directions and is lower than for the purely parallel case by a factor of hundred. Therefore we adopt here the value $\eta \sim 10^{-4}$ for the injection parameter (Völk et al. 2002).

According to our above estimate a substantial part of the shock still efficiently injects and accelerates CRs. This fraction is effectively increased relative to the above percentage due to broadening of the injection region by the strong wave field as well as by CR diffusion perpendicular to the mean magnetic field. In addition, the overall conservation equations ensure an approximately spherical character of the overall dynamics. Therefore, we assume the spherically symmetric approach for the nonlinear particle acceleration process to be approximately valid in those shock regions where injection is efficient. To take the effective injection fraction $f_{\text{re}} < 1$ into account, we need then to introduce a renormalization factor for the CR acceleration efficiency and for all the effects which it produces in the SNR. A rough estimate of its value is $f_{\text{re}} = 0.15 \div 0.25$.

Note that such a picture is consistent with the observed structure of SN 1006: the intense radio and X-ray emissions come from two bright rims with radially oriented magnetic field (Reynolds & Gilmore 1993). They may be the polar regions of a quasispherical shock in an outer magnetic field. The γ -ray observations may indicate a similar asymmetry (Tanimori et al. 1998) which would be well explained by a corresponding concentration of CR nucleons towards the polar regions.

We assume that electrons are also injected into the diffusive shock acceleration process still at nonrelativistic energies below $m_e c^2$. Since the electron injection mechanism is not very well known (e.g. Malkov & Drury 2001) for simplicity we consider their acceleration starting from the same momentum as protons. At relativistic energies they have exactly the same dynamics as the protons. Therefore, neglecting synchrotron losses, their distribution function at any given time has the form

$$f_e(p) = K_{\text{ep}} f(p) \quad (2)$$

for energies exceeding the electron injection energy, with some constant factor K_{ep} which is about 10^{-2} for the average CRs in the Galaxy. We take it here as a parameter.

The electron distribution function $f_e(p)$ deviates only at sufficiently large momenta from this relation due to synchrotron losses, which are taken into account by supplementing the ordinary diffusive transport equation by a loss term:

$$\frac{\partial f_e}{\partial t} = \nabla \kappa \nabla f_e - \mathbf{w} \nabla f_e + \frac{\nabla \mathbf{w}}{3} p \frac{\partial f_e}{\partial p} - \frac{1}{p^2} \frac{\partial}{\partial p} \left(\frac{p^3}{\tau_1} f_e \right), \quad (3)$$

where the first three terms in the right hand side of this equation describe diffusion, convection due to the mass velocity \mathbf{w} of the gas and adiabatic effects, respectively. The synchrotron loss time in the third term is determined by the expression (e.g. Berezhinskii et al. 1990)

$$\tau_1 = \left(\frac{4r_0^2 B^2 p}{9m_e^2 c^2} \right)^{-1}, \quad (4)$$

where m_e is the electron mass and r_0 the classical electron radius.

The solution of the dynamic equations at each instant of time yields the CR spectrum and the spatial distributions of CRs and gas. This allows us to calculate the expected flux $F_{\gamma}^{\text{pp}}(\epsilon_{\gamma})$ of γ -rays from π^0 -decay due to hadronic (p-p) collisions of CRs with the gas nuclei (e.g. Berezhko & Völk 1997).

The choice of K_{ep} allows us to determine in addition the electron distribution function and to calculate the associated emission. The expected synchrotron flux at distance d from the SNR is given by the expression (e.g. Berezhinskii et al. 1990)

$$S_{\nu} = \frac{3 \times 10^{-21}}{d^2} \int_0^{\infty} dr r^2 B_{\perp} \int_0^{\infty} dp p^2 f_e(r, p) F\left(\frac{\nu}{\nu_c}\right) \quad (5)$$

in $\text{erg}/(\text{cm}^2 \text{s})$, where

$$F(x) = x \int_x^{\infty} K_{5/3}(x') dx',$$

$K_{\mu}(x)$ is the modified Bessel function, $\nu_c = 3eB_{\perp} p^2 / [4\pi(m_e c)^3]$ and B_{\perp} is the magnetic field component perpendicular to the line of sight.

Since in the shock region where particle injection and acceleration is efficient the upstream magnetic field is assumed to be almost completely randomized due to intense Alfvén wave generation we approximate the post-shock magnetic field B_2 by $B_2 = \sigma B_0$, taking into account that the perpendicular field component undergoes amplification due to the gas compression at the shock front. We suggest also that in such a young SNR like SN 1006 the downstream magnetic field B_d in a relatively thin region between the shock and the ejecta is approximately uniform: $B_d = B(r < R_s) = B_2$.

The relativistic electrons produce γ -ray emission due to inverse Compton (IC) scattering of background photons. It is not difficult to show that due to the hard spectrum of accelerated electrons only the 2.7 K cosmic microwave background is important in the case considered. The expected differential flux of IC γ -rays as a function of their energy ϵ_{γ} can be represented in the form:

$$\begin{aligned} \frac{dF_{\gamma}^{\text{IC}}}{d\epsilon_{\gamma}} &= \frac{4\pi c}{d^2} \int_0^{\infty} dr r^2 \int_0^{\infty} d\epsilon n_{\text{ph}}(\epsilon) \\ &\times \int_{p_{\text{min}}}^{\infty} dp p^2 \sigma(\epsilon_e, \epsilon_{\gamma}, \epsilon) f_e(r, p) \end{aligned} \quad (6)$$

in $\text{photons}/(\text{cm}^2 \text{s erg})$, where (Blumenthal & Gould 1970)

$$\sigma(\epsilon_e, \epsilon_{\gamma}, \epsilon) = \frac{3\sigma_T(m_e c^2)^2}{4\epsilon_{\gamma}\epsilon_e}$$

$$\times \left[2q \ln q + (1 + 2q)(1 - q) + 0.5 \frac{(\Gamma q)^2(1 - q)}{1 + \Gamma q} \right] \quad (7)$$

is the differential cross section for the up-scattering of a photon with incident energy ϵ to energy ϵ_γ by the elastic collision with an electron of energy ϵ_e ,

$$n_{\text{ph}} = \frac{1}{\pi^2 (\hbar c)^3} \frac{\epsilon^2}{\exp(\epsilon/k_B T) - 1} \quad (8)$$

is the blackbody spectrum of the microwave background, \hbar and k_B are Planck and Boltzmann constant respectively, $T = 2.7$ K, $\sigma_T = 6.65 \times 10^{-25}$ cm² is the Thomson cross-section, $q = \epsilon_\gamma / [\Gamma(\epsilon_e - \epsilon_\gamma)]$, $\Gamma = 4\epsilon\epsilon_e / (m_e c^2)^2$, and p_{min} is the minimal momentum of electron, whose energy ϵ_e is determined by the condition $q = 1$.

3. Results and Discussion

Since SN 1006 is a type Ia SN we use typical SN Ia parameters in our calculations: ejected mass $M_{\text{ej}} = 1.4 M_\odot$, $k = 7$, and a uniform ambient ISM. We adopt a distance $d = 1.8$ kpc and the ambient number density of ISM hydrogen $N_{\text{H}} = 0.3$ cm⁻³, consistent with X-ray and optical imagery of SN 1006 (Winkler & Long 1997, see also Allen et al. 2001 and references therein). The value $T_0 = 10^4$ K is used for the ISM temperature. Note that SNR and CR dynamics are not sensitive to T_0 , because the shock structure is mainly determined by the Alfvénic Mach number.

We use an upstream magnetic field value $B_0 = 20$ μ G, which is required to provide the required shape of the synchrotron spectrum in the radio and X-ray bands.

The gas dynamic problem is characterized by the following length, time, and velocity scales:

$$R_0 = (3M_{\text{ej}}/4\pi\rho_0)^{1/3}, \quad t_0 = R_0/V_0, \quad V_0 = \sqrt{2E_{\text{sn}}/M_{\text{ej}}},$$

which are the sweep-up radius, sweep-up time and mean ejecta speed respectively. Here $\rho_0 = 1.4m_p N_{\text{H}}$ is the ISM mass density, m_p is the proton mass.

The shock expansion law during the free expansion phase ($t < t_0$) is then

$$R_s \propto E_{\text{sn}}^{(k-3)/2k} \rho_0^{-1/k} t^{(k-3)/(k-2)} \quad (9)$$

(Chevalier 1982) which for $k = 7$ gives

$$R_s \propto (E_{\text{sn}}/\rho_0)^{1/7} t^{4/5}. \quad (10)$$

In the adiabatic phase ($t \gtrsim t_0$) we have

$$R_s \propto (E_{\text{sn}}/\rho_0)^{1/5} t^{2/5}. \quad (11)$$

The observed expansion law of SN 1006 (Moffett et al. 1993) is $R_s \propto t^\mu$ with $\mu = 0.48 \pm 0.13$. One can conclude that within the observational errors SN 1006 should already be in the adiabatic phase.

The calculations together with the experimental data are shown in Fig.1–5. For the assumed SN distance and ISM density an explosion energy $E_{\text{sn}} = 3 \times 10^{51}$ erg fits the observed SNR size R_s and its expansion rate V_s (Moffett et al. 1993).

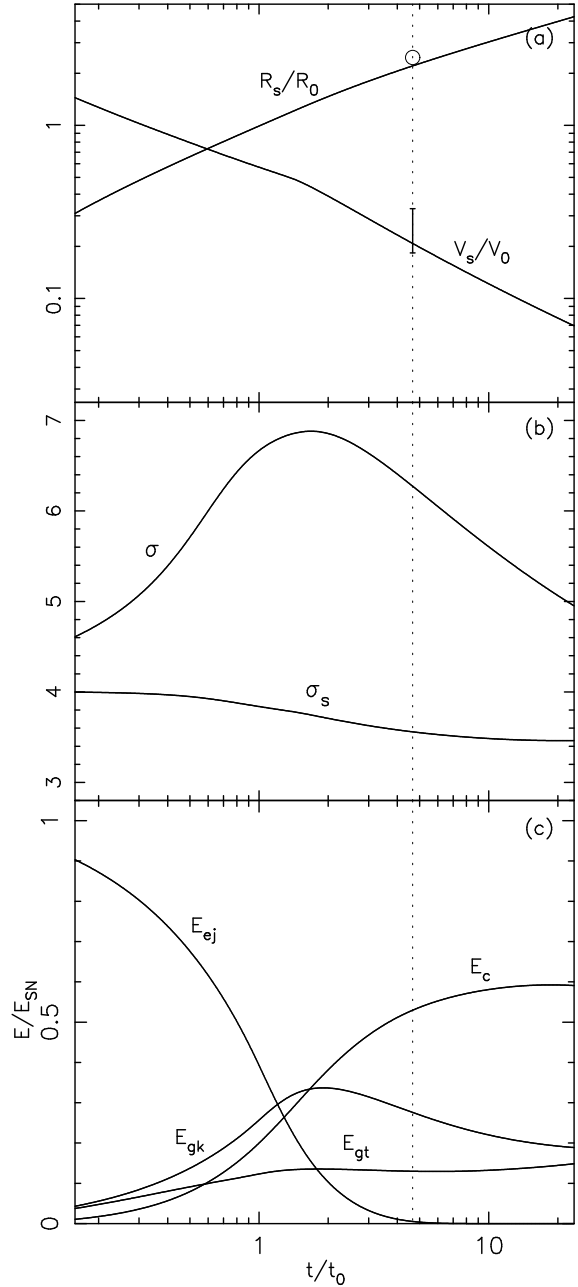


Fig. 1. (a) Shock radius R_s and shock speed V_s ; (b) total shock (σ) and subshock (σ_s) compression ratios; (c) ejecta (E_{ej}), CR (E_c), gas thermal (E_{gt}), and gas kinetic (E_{gk}) energies as a function of time. Scale values are $R_0 = 3.2$ pc, $V_0 = 14675$ km/s, $t_0 = 212$ years. The dotted vertical line marks the current epoch. The observed size and speed of the shock (Moffett et al. 1993), are shown as well.

According to Fig.1a SN 1006 is indeed already in the adiabatic phase. The assumed injection rate $\eta = 2 \times 10^{-4}$ leads to a significant modification of the shock which at the current epoch, $t = 995$ yr, has a total compression ratio $\sigma = 6.3$ and a subshock compression ratio $\sigma_s = 3.6$ (Fig.1b).

The different SNR energy components, the ejecta energy E_{ej} , the gas kinetic (E_{gk}), and thermal (E_{gt}) energies,

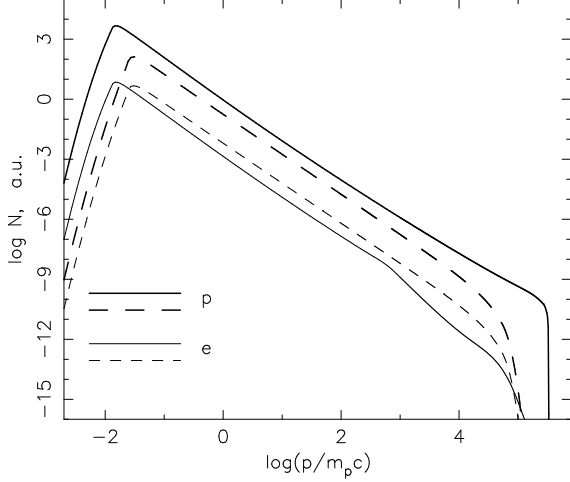


Fig. 2. The overall CR spectrum as function of momentum. Thick and thin lines correspond to protons and electrons, respectively. Solid and dashed lines correspond to efficient and inefficient proton acceleration, respectively.

and the CR energy E_c , are presented in Fig.1c as functions of time. The acceleration process is characterized by a high efficiency in spherical symmetry: at the current time $t/t_0 = 4.68$ about 45% of the explosion energy has been already transferred to CRs, and the CR energy content E_c continues to increase to a maximum of about 50% in the later Sedov phase (Fig.1c), when particles start to leave the source. As usually predicted by the model, the CR acceleration efficiency is significantly higher than required for the average replenishment of the Galactic CRs by SNRs, corresponding to $E_c \approx 0.1 E_{\text{sn}}$. As discussed before, this discrepancy can be attributed to the physical conditions at the shock surface which influence the injection efficiency. The magnetic field geometry is the most important factor: at the quasiperpendicular portion of the shock ion injection (and subsequent acceleration) is presumably depressed compared with the quasiparallel portion. Therefore the number of CRs, calculated within the spherically-symmetrical approximation, should be renormalized by this depression factor (see Völk et al. 2002 for details). Assuming SN 1006 to be an average Galactic CR source, the renormalizing factor should be $f_{\text{re}} = 0.2$. It means that according to our calculation the actual energy of accelerated protons in SN 1006 is

$$E_c = 0.45 f_{\text{re}} E_{\text{sn}} = 2.7 \times 10^{50} \text{ erg.} \quad (12)$$

Note that such a factor is consistent with observations which show that efficient CR acceleration takes place at about 25% of the shock surface (e.g. Allen et al. 2001).

The volume-integrated (or overall) CR spectrum

$$N(p, t) = 16\pi^2 p^2 \int_0^\infty dr r^2 f(r, p, t) \quad (13)$$

has, for the case of protons, almost a pure power-law form $N \propto p^{-\gamma}$ over a wide momentum range from $10^{-2} m_p c$ up to the cutoff momentum $p_{\text{max}} = \epsilon_{\text{max}}/c$, where $\epsilon_{\text{max}} \approx$

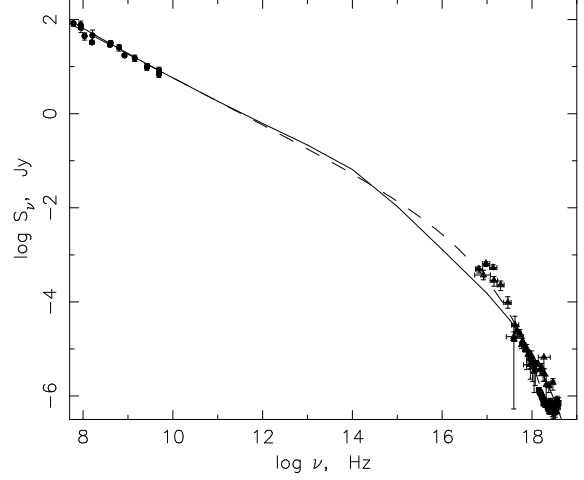


Fig. 3. Synchrotron emission flux as a function of frequency for the same two cases as in Fig.2. The observed X-ray (Hamilton et al. 1986; Allen et al. 1999) and radio emissions (Reynolds 1996) are shown.

3×10^{14} eV is the maximum CR energy (Fig.2). This value p_{max} is limited mainly by geometrical factors, which are the finite size and speed of the shock, its deceleration and the adiabatic cooling effect in the downstream region (Berezhko 1996). Due to the shock modification the power-law index slowly varies from $\gamma = 2.1$ at $p \lesssim m_p c$ to $\gamma = 1.8$ at $p \gtrsim 10^3 m_p c$.

The shape of the overall electron spectrum $N_e(p)$ deviates from that of the proton spectrum $N(p)$ at high momenta $p > p_1 \approx 10^3 m_p c$, due to the synchrotron losses in the downstream region with magnetic field $B_d \approx 120 \mu\text{G}$ which is assumed uniform in this region ($B_d = B_2 = \sigma B_0$). According to expression (4) the synchrotron losses become important for electron momenta greater than

$$\frac{p_1}{m_p c} \approx 1.3 \left(\frac{10^8 \text{ yr}}{t} \right) \left(\frac{10 \mu\text{G}}{B_d} \right)^2. \quad (14)$$

Substituting the SN age $t = 10^3$ yr into this expression, we have $p_1 \approx 600 m_p c$, in good agreement with the numerical results (Fig.2).

The shock constantly produces the electron spectrum $f_e \propto p^{-4}$ up to the maximum momentum p_{max}^e which is much larger than p_1 . Therefore, within the momentum range $p_1 \div p_{\text{max}}^e$, the electron spectrum is $f_e \propto p^{-5}$ due to synchrotron losses, and the corresponding overall electron spectrum is $N_e \propto p^{-3}$.

The maximum electron momentum can be estimated by equating the synchrotron loss time (4) and the acceleration time

$$\tau_a = \frac{3}{\Delta u} \left(\frac{\kappa_1}{u_1} + \frac{\kappa_2}{u_2} \right), \quad (15)$$

where $u_1 = V_s$ and $u_2 = u_1/\sigma$ are the upstream and downstream gas velocities relative to the shock front, and $\Delta u = u_1 - u_2$. During the acceleration time τ_a the electrons spent the time $3\kappa_1/(u_1 \Delta u)$ in the upstream mag-

netic field B_0 , and $3\kappa_2/(u_2\Delta u)$ in the downstream magnetic field $B_2 = \sigma_B B_0$; in the case considered $\sigma_B = \sigma$). Therefore, in the general case the maximum electron momentum p_{\max}^e is a solution of the equation

$$\tau_a(p)^{-1} = [\tau_1^{-1}(B_0, p) + \tau_1^{-1}(B_2, p)\sigma/\sigma_B]/(1 + \sigma/\sigma_B), \quad (16)$$

which can be written in the form

$$\frac{p_{\max}^e}{m_p c} = 6.7 \times 10^4 \left(\frac{V_s}{10^3 \text{ km/s}} \right) \times \sqrt{\frac{(\sigma - 1)}{\sigma(1 + \sigma_B \sigma)}} \left(\frac{10 \mu\text{G}}{B_0} \right). \quad (17)$$

The main part of the electrons with the highest energies $\epsilon_e \gtrsim 10$ TeV is produced at the end of the free expansion phase. At this stage $V_s \sim V_0$ which leads to a maximum electron momentum $p_{\max}^e \approx 4 \times 10^4 m_p c$ in agreement with the numerical results (Fig.2).

The parameter $K_{\text{ep}} = 1.5 \times 10^{-3}$ and $B_{\perp} = 0.3 B_d \approx 36 \mu\text{G}$ provide good agreement between the calculated and the measured synchrotron emission in the radio- and X-ray ranges (Fig.3). The steepening of electron spectrum at high energies due to synchrotron losses naturally yields a fit to the X-ray data with their soft spectrum. Note that two kinds of X-ray data are presented in Fig.3. The Hamilton et al. (1986) data represent the total X-ray emission in a relatively wide frequency range, where the non-thermal synchrotron emission contribution dominates at frequencies $\nu \gtrsim 10^{18}$ Hz. At these highest frequencies the Allen et al. (1999) nonthermal data are also presented, lying slightly below the Hamilton et al. data points. Clearly our model spectra must lie below the Hamilton et al. spectral points at $\nu \lesssim 10^{18}$ Hz. Such a smooth spectral behavior is achieved in a $20 \mu\text{G}$ upstream field.

Since the total number of accelerated protons has to be reduced by the factor $f_{\text{re}} = 0.2$, the same number of accelerated electrons then corresponds to the renormalized parameter $K_{\text{ep}} = 8 \times 10^{-3}$ that corresponds very well to the electron to proton ratio in the Galactic CRs. Then the total energy of accelerated electrons in SN 1006 is $E_c^e = 2 \times 10^{48}$ erg.

The radio data are fitted with the power law spectrum $S_{\nu} \propto \nu^{-\alpha}$, whose index $\alpha = 0.57 \pm 0.06$ (Allen et al. 2001) is noticeably larger than 0.5, corresponding to the electron spectrum $N_e \propto p^{-2}$ produced by an unmodified shock with compression ratio $\sigma = 4$. In our case the shock is essentially modified by the backreaction of the accelerated protons (see Fig.1b): its compression ratio $\sigma = 6.3$. At the same time low energy electrons with momenta $p \lesssim 10 m_p c$ ($\epsilon_e \lesssim 10$ GeV), which produce synchrotron emission at $\nu \lesssim 10$ GHz, are accelerated at the subshock which has the compression ratio $\sigma_s = 3.6$. Therefore these electrons have a steeper spectrum $N_e \propto p^{-2.1}$ that leads to the expected radio spectrum $S_{\nu} \propto \nu^{-0.54}$, fitting the experimental data very well (Fig.3). The fact that the observed value of the radio power law index α exceeds the value 0.5 can be considered as an indication that the shock is

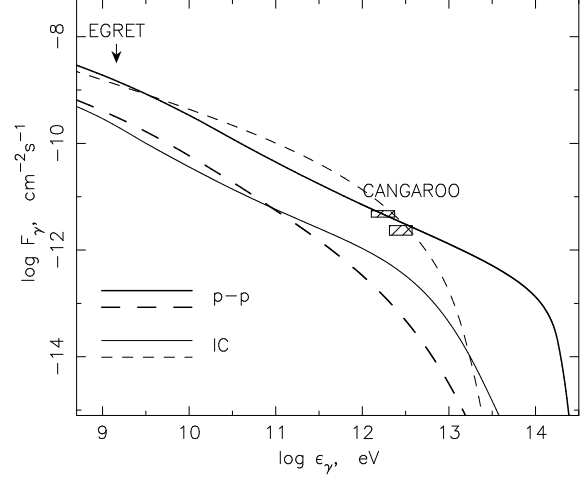


Fig. 4. IC (thin lines) and π^0 -decay (thick lines) γ -ray integral fluxes as a function of γ -ray energy for the same cases as in Fig.2. High energy γ -ray data (Tanimori et al. 1998) and the EGRET upper limit (Mastichiadis & de Jager 1996) are shown.

essentially modified. A relatively high upstream magnetic field strength $B_0 = 20 \mu\text{G}$, compared with typical ISM values $B_0 = 5 \mu\text{G}$, and a corresponding downstream value $B_{\perp} = 36 \mu\text{G}$ are required to have radio emitting electron energies in the steep part of their spectrum $\epsilon_e \lesssim 1$ GeV, and to give a smooth cutoff in the synchrotron spectrum $S_{\nu}(\nu)$ at frequencies $\nu = 10^{15} \div 10^{18}$ Hz. According to model calculations by Lucek and Bell (2000), the existing ISM field can be significantly amplified near the shock by CR streaming. We note the Bohm diffusion is consistent with such field amplification.

The calculated IC and π^0 -decay γ -ray fluxes are presented in Fig.4,5 together with existing experimental data. Note that the number of accelerated protons, which produce π^0 -decay γ -rays, is reduced by the factor $f_{\text{re}} = 0.2$.

According to the calculation, the hadronic γ -ray production exceeds the electron contribution by a factor of about 7 at energies $\epsilon_{\gamma} \lesssim 1$ TeV, and dominates at $\epsilon_{\gamma} > 10$ TeV (Fig.4). The calculation is in reasonable agreement with the TeV-measurements reported by the CANGAROO collaboration (Tanimori et al. 1998), and it does not contradict the EGRET upper limit $F_{\gamma}^E = 8 \times 10^{-9} \text{ cm}^{-2} \text{ s}^{-1}$ at $\epsilon_{\gamma} = 1.4$ GeV (cf. Mastichiadis & de Jager 1996). This is also confirmed by Fig.5, where we compare our calculations with the revised CANGAROO data (Tanimori et al. 2001). Compared with the measured γ -ray differential flux $dF_{\gamma}/d\epsilon_{\gamma}$, the calculated flux $dF_{\gamma}^{\text{pp}}/d\epsilon_{\gamma}$ is somewhat harder. However the discrepancy between the theory and experiment is not very relevant if one takes into account the experimental uncertainties which make the two highest points quite uncertain.

The γ -ray spectra produced by the electronic and hadronic CR components have closely similar shapes in the energy interval $1 \text{ GeV} \lesssim \epsilon_{\gamma} \lesssim 1 \text{ TeV}$ due to electron synchrotron losses. Therefore, the only observational pos-

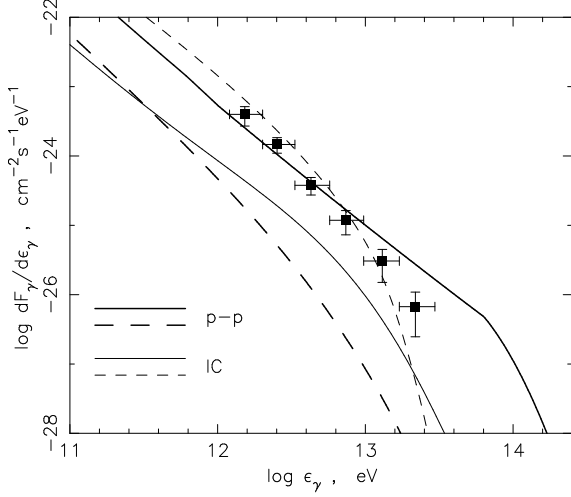


Fig. 5. Differential π^0 -decay (thick line) and IC (thin line) γ -ray flux as a function of γ -ray energy for the same cases as in Fig. 2. High energy γ -ray data (Tanimori et al. 2001) are shown.

sibility to discriminate between leptonic and hadronic contributions is to measure the γ -ray spectrum at energies essentially higher than 1 TeV, where these two spectra are expected to be essentially different. The detection of a substantial flux at energies $\epsilon_\gamma \gtrsim 10$ TeV would provide direct evidence for its hadronic origin.

4. Inefficient proton acceleration model

The set of parameters which was discussed until now is limited by the existing measurements. There is almost no freedom for a substantial change of any parameter value without a loss of agreement between theory and experiment. For example the proton injection rate, which determines the number of accelerated protons and the π^0 -decay γ -ray emission, is taken to produce the shock modification required to produce a steep electron spectrum $N_e \propto p^{-2.1}$ needed to fit the observed radio emission of SN 1006. For this injection rate $\eta = 2 \times 10^{-4}$ and electron to proton ratio $K_{ep} \sim 10^{-2}$ a relatively high upstream magnetic field is unavoidably required in order to produce the observed synchrotron emission.

On the other hand, one can dismiss the relevance of a deviation of the radio spectrum from the form $S_\nu \propto \nu^{-0.5}$ and try to reproduce all the observed emissions by effects of electrons alone (e.g. Pohl 1996; Mastichiadis & de Jager 1996; Yoshida & Yanagita 1997). The number of injected and accelerated protons and all the effects which they can produce in SN 1006 is suggested to be negligibly small in this extreme case. For example, the proton contribution to the TeV γ -ray emission should be at least an order of magnitude lower compared with the previous case. At such low proton numbers the nonlinear shock modification due to their backreaction is negligible, and shock acceleration takes place in the test particle limit.

In order to make clear how different the required set of relevant physical parameters compared to the case of efficient CR nucleon acceleration is, we performed a calculation which corresponds to inefficient CR acceleration. We use a proton injection rate $\eta = 10^{-5}$ which yields an upper limit for the proton acceleration efficiency that is consistent with their low contribution to the γ -ray production. This low CR nucleon production efficiency also implies that the effect of magnetic field amplification due to CR streaming is small. Therefore we have used a typical ISM magnetic field strength $B_0 = 4 \mu\text{G}$. Note also that such a low value was assumed to be required in the downstream region – $B_\perp = 4 \mu\text{G}$ – to fit the experimental data (Tanimori et al. 2001). All other ISM and SN parameters are the same as in the previous case of efficient CR acceleration. Since during the early evolutionary phase the global SNR dynamics is rather insensitive to the number of accelerated CRs, the observed SNR size and its expansion rate are equally well reproduced in this case.

In this test particle regime the electron spectrum, produced by a strong unmodified shock, has the approximate form (Berezhko 1996)

$$N_e \propto p^{-\gamma} \exp[-\kappa(p)/\kappa(p_{\text{max}}^e)], \quad (18)$$

with $\gamma \approx 2$, where p_{max}^e is the maximum CR momentum, which is determined by geometrical factors. For a Bohm-type diffusion coefficient, $\kappa \propto p$, the cutoff region of this spectrum has the same form $N_e \propto \exp(-p/p_{\text{max}}^e)$ as it was suggested by Mastichiadis & de Jager (1996) and by Tanimori et al. (2001). At the same time, cf. eq. (18), the spectrum of the electrons accelerated at a strong unmodified shock is essentially harder compared to what was used ($\gamma = 2.2$) to fit the radio, X-ray and γ -ray data (Tanimori et al. 2001). It is clear that the spectrum, cf. eq. (18), with $\gamma = 2$, which has the same number of GeV electrons to produce the same radio flux, has an order of magnitude more electrons with $\epsilon_e = 10$ TeV compared with the case $\gamma = 2.2$. Therefore, to fit the radio, X-ray, and γ -ray data with this harder electron spectrum, we need a large downstream magnetic field $B_\perp \approx 13 \mu\text{G}$. Since even for $\eta = 10^{-5}$ nucleon acceleration can produce a strong Alfvénic wave field, the upper limit for the downstream field strength B_d equals $16 \mu\text{G}$. To this extent $B_\perp \approx 13 \mu\text{G}$ can still be consistent with a $4 \mu\text{G}$ ISM magnetic field as used by Tanimori et al. (2001), although these authors used $4 \mu\text{G}$ also downstream.

Since the energies $\epsilon_e \gtrsim 10^{13}$ eV of electrons, whose synchrotron emission in the given magnetic field corresponds to X-ray energies $\epsilon_\nu > 5$ keV, should be in the exponential cutoff region, the required value of the maximum CR momentum is $p_{\text{max}}^e = 10^4 m_{pc}$. If we assume the same momentum dependence $\kappa \propto p$, this maximum CR momentum is consistent with the diffusion coefficient

$$\kappa(p) = 5.3 \kappa_{\text{Bohm}}(p), \quad (19)$$

which exceeds the Bohm limit by a factor 5.3 for an upstream field of $4 \mu\text{G}$.

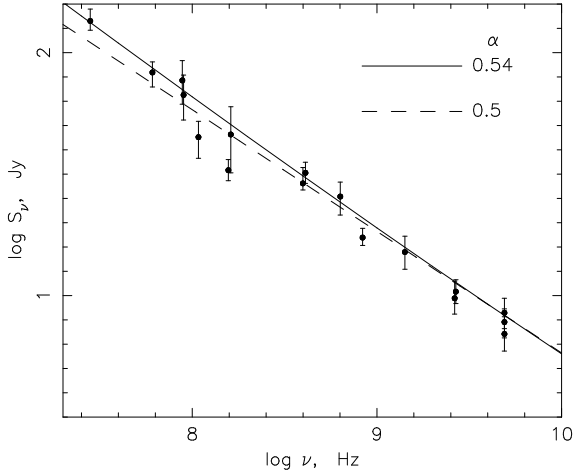


Fig. 6. Observed total radio flux of SN 1006 (Reynolds 1996) as a function of frequency with model spectra superimposed. Solid and dashed curves correspond to the high and low proton injection/acceleration efficiency, respectively.

The results for this inefficient proton injection/acceleration case are also presented in Fig.2–7. One can see from Fig.2 that, due to the lower magnetic field value, one needs about five times more accelerated electrons compared with the previous case to fit the radio and X-ray data (see Fig.3).

In this case the γ -ray production is dominated by the electron contribution (Fig.4), whose IC spectrum is essentially harder than in the previous case. The differential γ -ray CANGAROO spectrum appears in a better agreement with the inefficient model prediction than with the efficient one (Fig.5). But the rather large experimental uncertainties, especially of the last two points does not allow to discriminate between the two possibilities.

In Fig.6 the calculated synchrotron fluxes are compared with the experimental data in the radio range. One can see that the steeper spectrum $S_\nu \propto \nu^{-0.54}$ which corresponds to the efficient CR acceleration case gives a better fit to the radio data than the spectrum $S_\nu \propto \nu^{-0.5}$ corresponding to the case of inefficient proton injection, even though the experimental accuracy does not very clearly distinguish between these two variants. Note that $\alpha = 0.54$ is the average value of the power-law index within the frequency range shown in Fig.6. In fact due to the concave shape of the electron spectrum the index slightly decreases with increasing frequency, with $\alpha = 0.56$ and $\alpha = 0.51$ at the lowest and largest frequency respectively.

A similar situation is encountered in the X-ray range. An essentially steeper electron spectrum in the case of efficient CR accelerations much better fits the X-ray data (Fig.3).

At given number of protons and magnetic field strength an electron to proton ratio $K_{ep} = 0.2$ is required in the inefficient case, in order to reproduce the observed emission. This value is about 50 times larger than for the Galactic CRs.

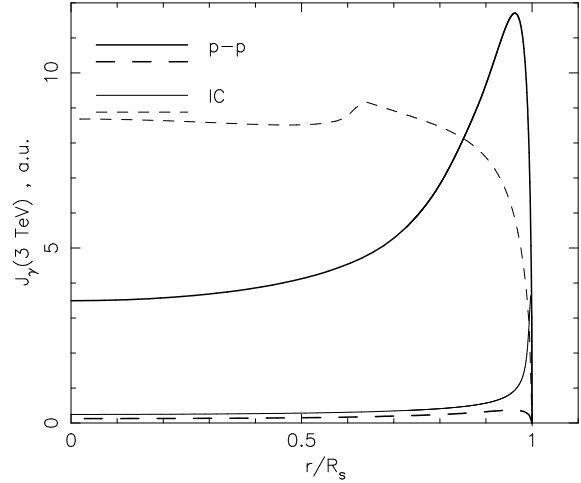


Fig. 7. Radial dependence of the γ -ray brightness for the γ -ray energy $\epsilon_\gamma = 3$ TeV. Solid and dashed curves correspond to the high and low proton injection/acceleration efficiency, respectively.

Nucleonic CRs absorb in this case only

$$E_c = 0.008 E_{sn} = 2.4 \times 10^{49} \text{ erg}, \quad (20)$$

which is more than an order of magnitude less than required for the Galactic CRs. The electron CR component contains $E_c^e = 5 \times 10^{48}$ erg. This is a factor 1.4 less than what has been obtained by Dyer et al. (2001) corresponding due to their lower downstream magnetic field of $9 \mu\text{G}$.

It is important to note that the γ -ray brightness of the remnant

$$J_\gamma(\epsilon_\gamma, r) \propto \int dx q_\gamma(\epsilon_\gamma, r, x) \quad (21)$$

has a very different dependence upon the distance from its center r in the two considered cases. The integration of the γ -ray luminosity q_γ in the above expression is performed along the line of sight which intersects the visible remnant surface at the projected distance r from its center. In the case of inefficient proton injection TeV γ -rays are produced by the electrons with the highest energies of their spectrum $\epsilon_e \gtrsim \epsilon_{\max}^e$. These electrons almost uniformly occupy the entire volume between the shock surface R_s and the contact discontinuity R_p which separates the ejecta and swept-up matter almost uniformly. Depending on the turbulence level near the contact discontinuity they also partially fill the ejecta volume $r \lesssim R_p$. Therefore the TeV γ -ray brightness $J_\gamma(r)$ will have a peak value at $r = R_p$ if particle penetration through the contact discontinuity is strongly suppressed, and at the center of the remnant $r = 0$ in the opposite case.

A significantly different radial profile $J_\gamma(r)$ is expected in the case of efficient proton production. TeV γ -rays are produced in this case by protons whose energy is considerably lower than the cutoff energy ϵ_{\max} . Therefore they are concentrated within the thin region of thickness $\Delta r \approx R_s/(3\sigma)$ just behind the shock. The swept-up gas

has a similar distribution. Since the π^0 -decay γ -ray luminosity is proportional to the product of the CR density and the gas number density, the γ -ray brightness $J_\gamma(r)$ is expected to have a sharp peak close to the shock edge $r \approx R_s$ with a considerable decrease at small distances $r \ll R_s$.

The γ -ray brightness calculated for the two different cases is presented in Fig.7 for the γ -ray energy $\epsilon_\gamma = 3$ TeV. One can see the essentially different radial dependence $J_\gamma(r)$ for the two cases. The γ -rays of hadronic origin are expected to be concentrated in the postshock region, whereas the IC γ -ray brightness, calculated for quite a large level of turbulence near the contact discontinuity (see Berezhko & Völk 2000 for details), is almost uniformly distributed across the visible disk of the remnant.

The reported γ -ray flux was detected from the same outer part of SN 1006 which shows the radio-emission. This can be considered as an observational argument favoring a strong role for the nuclear CR component.

5. Summary

The nonlinear kinetic model for CR acceleration in SNRs has been applied to SN 1006 in order to explain its observed properties. We have used stellar ejecta parameters $M_{ej} = 1.4M_\odot$, $k = 7$, distance $d = 1.8$ kpc, and ISM number density $N_H = 0.3 \text{ cm}^{-3}$ from X-ray and optical imaginary of SN 1006.

For these parameters the explosion energy $E_{sn} = 3 \times 10^{51}$ erg is required to fit the observed size R_s and expansion speed V_s which are determined by the ratio E_{sn}/N_H .

The number of accelerated electrons required to fit the radio and X-ray emission of SN 1006, and correspondingly the role of accelerated protons in γ -ray production, depends essentially on the magnetic field value B_0 .

It was demonstrated that for low magnetic field $B_0 = 4 \mu\text{G}$ all the observed emissions are dominated by the electron contribution. Protons are then assumed to be injected into the acceleration much less efficiently than electrons so that the lowest permitted value of electron to proton ratio is $K_{ep} = 0.2$. It is much larger than observed in the Galactic CRs. The maximum energy of accelerated CRs and their total energy content in this case are only $\epsilon_{max} \sim 10^{13}$ eV and $E_c \lesssim 10^{49}$ erg respectively. These numbers are too low for such SNRs to be considered as the main sources of the Galactic CRs.

If CRs in SN 1006 are produced due to the diffusive shock acceleration process, then even in the case of inefficient proton injection quite a large downstream magnetic field $B_d \approx 13 \mu\text{G}$ is required to fit the data. It is several times larger than in a simple estimate (Tanimori et al. 2001) because the shock produces in this case an electron spectrum $N_e \propto \epsilon_e^{-2}$ that is significantly harder than was assumed in a simple estimate.

The existing data are better approximated if a significantly larger upstream magnetic field value $B_0 = 20 \mu\text{G}$ and a physically much more plausible efficient nucleon injection are assumed. The required magnetic field strength,

that is significantly higher than the rms value $5 \mu\text{G}$ in the ISM, might be the result of non-linear amplification near the SN shock by the CR acceleration process itself.

We find that after adjustment of the predictions of the nonlinear spherically-symmetric model by a renormalization of the number of accelerated nuclear CRs to take account of the large area of quasiperpendicular shock regions of a SNR, good consistency with all observational data can be achieved, including the reported TeV γ -ray flux.

The π^0 -decay γ -ray flux produced by the nuclear CR component exceeds the flux of IC γ -rays generated by the electronic CR component at 1 TeV. Therefore the reported TeV flux from SN 1006 supports the idea that the nuclear CR component is indeed produced in SNRs.

The expected π^0 -decay γ -ray flux $F_\gamma \propto \epsilon_\gamma^{-1}$ extends up to 100 TeV, whereas the IC γ -ray flux has a cutoff above a few TeV. Therefore the detection of γ -ray emission above 10 TeV would imply evidence for a hadronic origin.

The maximum accelerated proton energy $\epsilon_{max} = 3 \times 10^{14}$ eV, their energy content $E_c \approx 3 \times 10^{50}$ erg and electron to proton ratio $K_{ep} \approx 10^{-2}$ reproduced in this case are consistent with the requirements for the Galactic CR sources.

Unfortunately the quality of the existing data does not allow a clear empirical conclusion which of these two very different scenarios is realized in SN 1006. To discriminate them one needs to measure the γ -ray flux at energies $\epsilon_\gamma \gtrsim 10$ TeV. The existence of γ -rays with such high energies will be a confirmation of the efficient CR production in SN 1006 with an electron to proton ratio and their acceleration efficiency consistent with the requirements on the Galactic CR energy budget.

Acknowledgements. This work has been supported in part by the Russian Foundation for Basic Research (grants 00-02-17728, 99-02-16325). EGB and LTK acknowledge the hospitality of the Max-Planck-Institut für Kernphysik, where part of this work was carried out.

References

- Aharonian, F.A. & Atoyan, A.M. 1999, A&A, 351, 33
- Allen, G.E., Gotthelf, E.V. & Petre, R. 1999, In 26th ICRC, Salt Lake City, vol. 3, 480
- Allen, G.E., Petre, R. & Gotthelf, E.V. 2001, ApJ, 558, 739
- Bennet, L. & Ellison, D.C. 1995, JGR, 100, 3439
- Berezhko, E.G. 1996, Astropart. Phys., 5, 367
- Berezhko, E.G., Elshin, V.K. & Ksenofontov, L.T. 1996, JETP, 82, 1
- Berezhko, E.G. & Völk, H.J. 1997, Astropart. Phys., 7, 183
- Berezhko, E.G. & Ellison, D.C. 1999, ApJ, 526, 385
- Berezhko, E.G., Ksenofontov, L.T. & Petukhov, S.I. 1999, In 26th ICRC, Salt Lake City, vol. 3, 431
- Berezhko, E.G. & Völk, H.J. 2000, A&A, 357, 283
- Berezhko, E.G., Ksenofontov, L.T. & Völk, H.J. 2001, In 27th ICRC, Hamburg, vol. 5, 2489
- Berezinskii, V.S., Bulanov, S.A., Dogel, V.A. et al. 1990, Astrophysics of cosmic rays, North-Holland: Publ.Comp.

- Blumenthal, G.R. & Gould, R.J. 1970, *Rev. Mod. Phys.*, 42, 236
- Chevalier, R.A. 1982, *ApJ*, 258, 790
- Drury, L.O'C., Aharonian, F.A. & Völk, H.J. 1994, *A&A*, 287, 959
- Dyer, K.K., Reynolds, S.P., Borkowski, K.J. et al. 2001, *ApJ*, 551, 439
- Ellison, D.C., Baring, M.G. & Jones, F.C. 1995, *ApJ*, 453, 873
- Jones, E.M., Smith, B.W. & Straka, W.C. 1981, *ApJ*, 249, 185
- Hamilton, A.J.S., Sarazin, C.L. & Szymkowiak, A.E. 1986, *ApJ*, 300, 698
- Koyama, K., Petre, R., Gotthelf, E.V. et al. 1995, *Nature*, 378, 255
- Lucek, S.G. & Bell, A.R. 2000, *MNRAS*, 314, 65
- Malkov, M.A. 1998, *Phys. Rev. E*, 58, 4911
- Malkov, M.A. & Völk, H.J. 1995, *A&A*, 300, 605
- Malkov, M.A. & Völk, H.J. 1996, *Adv. Space Res.*, 21, No. 4, 551
- Malkov, M.A. & Drury, L. O'C. 2001, *Rep. Prog. Phys.* 64, 429
- Malkov, M.A., Diamond, P.H. & Jones, T.W. 2001, to appear in *ApJ*, available as arXiv:astro-ph/0112046 v1 3 Dec 2001
- Mastichiadis, A. & de Jager, O.C. 1996, *A&A*, 311, L5
- Moffett, D.A., Goss, W.M. & Reynolds, S.P. 1993, *AJ*, 106, 1566
- Pohl, M. 1996, *A&A*, 307, L57
- Reynolds, S.P. 1996, *ApJ*, 459, L13
- Reynolds, S.P. & Gilmore, D.M. 1993, *AJ*, 92, 1138
- Scholer, M., Trattner, K.J. & Kucharek, H. 1992, *ApJ*, 395, 675
- Tanimori, T., Hayami, Y., Kamei, S. et al. 1998, *ApJ*, 497, L25
- Tanimori, T., Naito, T., Yoshida, T. et al., 2001. In 27th ICRC, Hamburg, vol. 5, 2465
- Trattner, K.J. & Scholer, M. 1994, *JGR*, 99, 6637
- Völk, H.J. et al., 2002, in preparation
- Winkler, P.F. & Long, K.S. 1997, *ApJ*, 491, 829
- Yoshida, T. & Yanadita, S. 1997, In 2nd INTEGRAL Workshop 'Transparent Universe' (ESA SP-382), 85